crystals

MDPI

Article

Pulsed Electrodeposition for Copper Nanowires

Duc-Thinh Vuong †, Ha-My Hoang †, Nguyen-Hung Tran and Hyun-Chul Kim *

High Safety Vehicle Core Technology Research Center, Department of Mechanical Engineering, Inje University, Gimhae-si 50834, Korea; vuongthinhbk@gmail.com (D.-T.V.); hamyhoang@kimm.re.kr (H.-M.H.); trannguyenhung.work@gmail.com (N.-H.T.)

* Correspondence: mechkhc@inje.ac.kr; Tel.: +82-55-320-3988; Fax: +82-55-324-1723

† These authors contributed equally to this work.

Received: 27 February 2020; Accepted: 17 March 2020; Published: 20 March 2020

Abstract: Copper nanowires (Cu NWs) are a promising alternative to indium tin oxide (ITO), for use as transparent conductors that exhibit comparable performance at a lower cost. Furthermore, Cu NWs are flexible, a property not possessed by ITO. However, the Cu NW-based transparent electrode has a reddish color and tends to deteriorate in ambient conditions due to the oxidation of Cu. In this paper, we propose a pulsed-current (PC) plating method to deposit nickel onto the Cu NWs in order to reduce oxidation over a 30-day period, and to minimize the sheet resistance. Additionally, the effects of the pulse current, duty cycle, and pulse frequency on the performance of the Cu–Ni (copper–nickel) NW films have also been investigated. As a result, the reddish color of the electrode was eliminated, as oxidation was completely suppressed, and the sheet resistance was reduced from 35 Ω/sq to 27 Ω/sq. However, the transmittance decreased slightly from 86% to 76% at a wavelength of 550 nm. The Cu–Ni NW electrodes also exhibited excellent long-term cycling stability after 6000 bending cycles. Our fabricated Cu–Ni electrodes were successfully applied in flexible polymer-dispersed liquid crystal smart windows.

Keywords: pulsed current plating; copper nanowire; nickel electrodeposition; polymer-dispersed liquid crystal-based smart windows; transparent electrode

1. Introduction

Recently, due to the increase in smart devices, such as smartphones, smart-glass, which is a conducting layer that facilitates charge transport without blocking the transmission of light, is in great demand. Metal nanowires (NWs) have proven to be the preferred materials to replace indium tin oxide (ITO) as flexible transparent conducting film electrodes, with a low sheet resistance and high transparency. As such, there have been many attempts to improve the synthesis, purification, and coating of these NWs [1]. Since their conductivity is comparable to that of silver nanowires (Ag NWs), copper nanowires (Cu NWs) are a promising alternative to ITO as future electrodes, because of the relative abundance of Cu and the low cost of the solution-phase NW synthesis process [2]. Moreover, flexible transparent electrodes from Cu NWs possess extremely robust mechanical properties that are not exhibited by ITO [3].

The oxidation of Cu NWs in ambient conditions has limited its use for many applications. Hence, there have been many attempts to enhance the oxidation suppression of Cu NWs, such as polymer over-coating [4], metal NW surface coating [5], graphene or reduced graphene oxide (RGO) coating [6], or using an aluminum-doped zinc oxide (AZO) layer [7]. Nickel is the most commonly used metal in the electroplating of Cu NW electrodes because the Ni coating forms an effective barrier against oxidation during exposure to air [8]. Nickel on the Cu NWs in an electrochemical workstation [9], as well as in a traditional Watt bath [10], plays an important role not only by protecting the Cu NWs in

an air or a water environment for a prolonged period, but also by filling the network of the Cu NWs, consequently reducing the sheet resistance. Moreover, when electroless Ni plating was conducted on the films of cupro-nickel NWs, they were 1000 times more resistant to oxidation than untreated Cu NW films; however, their transmittance was 10% lower than that of the Cu NW films at a sheet resistance of 60 Ω/sq [11].

In this paper, we propose a pulsed current (PC) plating technique to deposit nickel on the Cu NW electrodes using a traditional Watt bath electrolyte that is modified as in a previous report [10]. The effects of pulsed current parameters such as frequency, duty cycle, and current density have also been investigated. Transmission electron microscopy (TEM), and scanning electron microscopy (SEM) images clearly show the Cu core–Ni shell and surface of the Ni layer on the Cu NWs. Moreover, cracks in the network of the Ni-plated layer, which resulted in performance-related problems, also showed in the electron microscope images at different current densities. All the electrodes were exposed to ambient conditions and high temperatures for an extended period, to investigate the antioxidant effect. Finally, the Cu–Ni NW electrodes on apolyethylene terephthalate(PET) substrate exhibited excellent flexibility when applied in the flexible polymer-dispersed liquid crystal (PDLC) smart windows.

2. Materials and Methods

2.1. Materials

Acetic acid (1002−4400), isopropyl alcohol (IPA, 5035−4400), nickel (II) chloride hexahydrate ($NiCl_2{\cdot}6H_2O$, 5607−4400), nickel (II) sulfate hexahydrate ($NiSO_4{\cdot}6H_2O$, 5611−4400), and boric acid (H_3BO_3, 2036−4400) were purchased from Daejung Chemicals & Metals (Korea). Polyethylene terephthalate (PET) with a thickness of 50 μm was obtained from KAIST (Deajeon, Korea). Microscope slides (25 × 75 mm/ca. 1 mm) were procured from Heinz Herenz (Hamburg, Germany)

2.2. Copper Nanowire Transparent Conducting Film Preparation

Cu NWs were synthesized following our previous synthesis procedures [12]. The pure Cu NWs were then dispersed in 0.5 wt% poly(vinyl pyrrolidone) (PVP) in IPA for storage. To prepare Cu NW-based electrode, a desired amount of the stored Cu NWs was transferred to a 1.5 mL tube and washed once more with the 0.5 wt% of PVP-based ink solution. After dropping a volume of Cu NW ink on a substrate, a Meyer rod was pulled manually over the Cu NWs solution left a uniform layer. To activate the Cu NWs electrode, it was necessary to remove the PVP that covered the Cu NWs; the films were dipped in acetic acid for 5 min and quickly dried using a hairdryer.

2.3. Pulsed Plating

The typical plating bath consisted of a mix of 38.215 g of $NiSO_4{\cdot}6H_2O$, 5.502 g of $NiCl_2{\cdot}6H_2O$, 3.0 g of boric acid, and 100 mL of deionized (DI) water. The mixture was magnetically stirred at 700 rpm for 30 min for dissolution. A pure nickel bar was attached to the cathode, and the Cu NW electrode was connected to the anode using copper conducting tape. Both were dipped in the nickel-plating bath. Two data acquisition (DAQ) cards, namely NI-9223 and NI-9227, were attached to the circuit to monitor the applied voltage and the plating current. The plating process was initiated by turning on the power supply. The Cu NW films were deposited using direct current (DC) and pulsed current (PC) electrodeposition modes. Figure 1a,b symbolize the typical potential square wave signal and the corresponding current density respectively, as a function of time during the pulsed electrodeposition mode. From Figure 1, it can be seen that the shape of applied potential pulses are square; however, the corresponding current density is modulated differently, due to the presence of an electric double layer at the cathode electrolyte interface forming a capacitor of molecular dimensions [13,14]. After plating, the electrodes were rinsed with DI water and dried using a hairdryer.

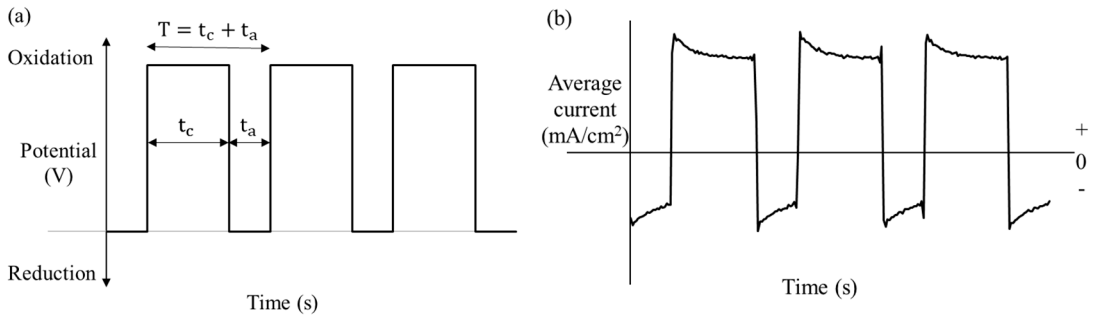

Figure 1. (**a**) Schematic representation of the pulse waveform for electrodeposition at duty cycle (ϕ) = $t_c/t_c + t_a$ = 67% (T: cycle time, t_c: cathodic (forward) time, t_a: anodic (reverse) time) (**b**) Current density as a function of time during the pulsed electrodeposition.

2.4. Flexible Smart Window Fabrication

Polymer-dispersed liquid crystal (PDLC) solution was obtained from Dong Gang University Incubator Center, Gwangju. Firstly, a tape of 0.5 mm thickness was applied to both sides of the Cu–Ni NW electrode on PET. Then, the copper tape was pasted to the top of the electrode to supply the conducting wires with power. Next, a pipette was used to place 50 mL of PDLC solution between the two Cu–Ni NWs films. The two glasses were put on two sides of the device while pressing so that the solution was distributed uniformly on the surface. Then, that device was placed in a UV chamber that had a UV light (365 nm) with a power of 4 W (Vilber Lourmat) at a distance of 10 cm from the sample; the irradiation process lasted 30 minutes. After curing, the film became translucent and the residual solution was cleaned Figure 2 shows the complete structure and demonstrates the operation of the PDLC smart window.

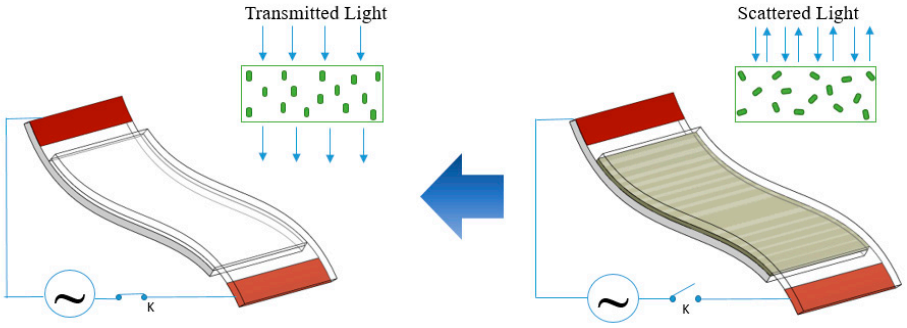

Figure 2. The schematic of the structure and operation of a Cu–Ni NW-based flexible PDLC smart window.

2.5. Characterization

The synthesized Cu NWs were analyzed using SEM (Hitachi S-4800) (Central Microscopy Research Facility, The University of Iowa, USA). X-ray diffraction (XRD) of the Cu NW samples was measured in the range of 2θ = 20–80° by step scanning on the X'Pert PRO MPD X-ray diffractometer of PANalytical (Malvern Panalytical, Malvern Worcestershire, WR14 1XZ United Kingdom). The optical specular transmittance of the electrode was measured using a T60 UV/VIS Spectrophotometer of PG Instruments Limited.

3. Results and Discussion

3.1. Pulsed Plating

Figure 3 shows the SEM images, which exhibited uniform, straight, and ultralong Cu NWs. The Cu NWs were synthesized following our previously reported methods [12] with dimensions of

D = 52.1 ± 6.6 nm and L ≥ 100 μm to give high aspect ratio NWs, i.e., length/diameter (L/D) > 2380. Transparent electrodes that were prepared using our Cu NWs demonstrated excellent optoelectronic performance, specifically in terms of sheet resistance (R_s) versus transmittance (%T): 7.3, 30, 58, and 100 Ω/sq at 72.4, 90, 94, and 97% respectively. These results are equivalent to, or even greater than, those of some transparent electrodes based on Cu nanofiber webs (50 Ω/sq at 90%) [15] and Cu NWs synthesized via the solution route (90 Ω/sq at 90%) [16].

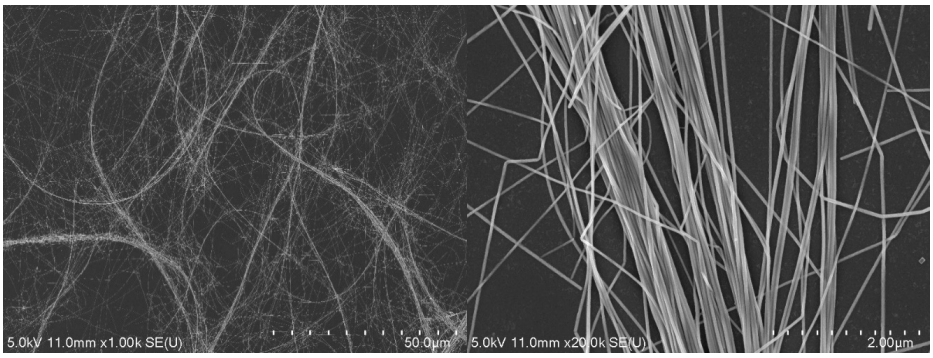

Figure 3. The Cu NWs were synthesized via a hexadecylamine (HDA)-mediated method. The NWs had a diameter of 55.3 ± 7.1 nm and a length greater than 100 μm.

The result of pulsed nickel electroplating is shown in Figure 4. The PC plating process successfully deposited nickel onto the Cu NWs. The SEM images in Figure 4a,b show Cu NWs before and after nickel PC plating, respectively. The diameter of the wires increased from 52.1 ± 6.6 nm to 77.1 ± 6.5 nm due to the deposition of nickel on the wires. This increase in diameter is a major contributor to the increase in light scattering and light absorption, which is probably responsible for the decline in transparency of the electrodes. On the other hand, as illustrated in the schematic in Figure 4c, after being plated, it appears that the nickel completely covered the NWs and junctions. The nickel atoms deposited at the intersection of two crossing wires would play a vital role in affecting the stability of the Cu NWs. This strengthened link created a solid network and significantly improved conductivity.

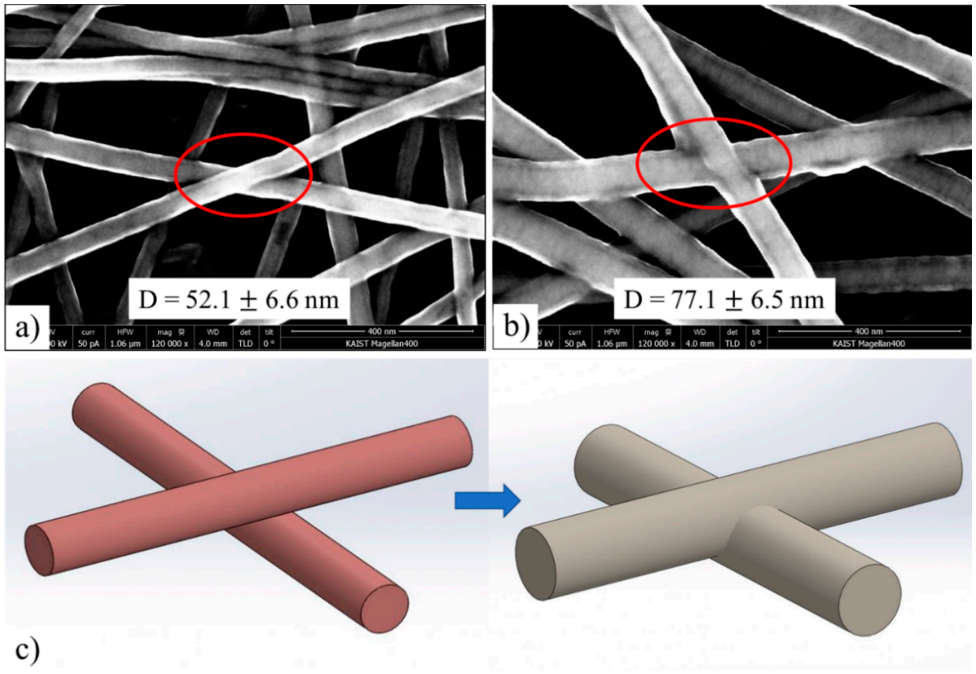

Figure 4. (**a**) CuNWs before, (**b**) after PC plating of nickel, (**c**) schematic of the intersection between two NWs before and after plating.

As shown in Figure 5a, energy-dispersive X-ray spectroscopy (EDS) images at a scale of 500 nm showed that the Cu and Ni elements on the sample are extracted from the Cu–Ni electrode after plating by PC. The green line of the Ni element coincided with the violet line of the Cu element, demonstrating that the Ni particles only deposited on the copper wires. Moreover, this is confirmed by the TEM images in Figure 5b of one Cu nanowire after PC plating at a 100 nm scale. The inset shows the Ni shell and Cu core and clearly demonstrates that the Cu nanowires are completely covered by Ni. The outer Ni layer protects the Cu NW by preventing direct contact with the oxygen in the air, hence reducing the rate of oxidation for several days which will be shown subsequently.

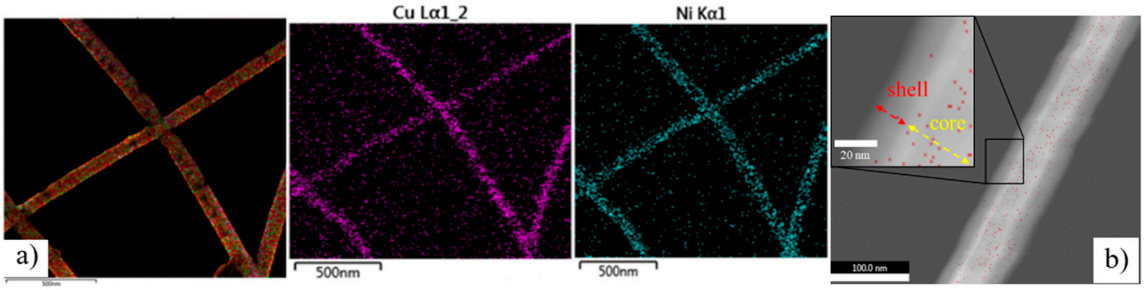

Figure 5. (**a**) EDS and (**b**) TEM images of the Cu–Ni nanowire network after plating.

3.2. Influence of Frequency and Duty Cycle on Nickel Deposition

The original Cu NWs (Figure 6a) had diameters of 52.1 ± 6.6 nm. Figure 6b–e shows the SEM images of nickel-pulsed electrodeposits under supplied power generated of 0–3 V; the duty cycle was 50%, the plating time was kept constant at 90 s, and the frequencies were 50 Hz, 100 Hz, 200 Hz, and 800 Hz. Figure 6e indicates the diameters of the Ni-coated Cu NWs as measured by ImageJ, and the crystallite size (grain size) was determined using the Scherrer equation utilizing the peak broadening of the (111) diffraction peak:

$$\beta = 0.94\lambda/(d \cdot \cos\theta) \quad (1)$$

The SEM images presented above demonstrate that the Ni coating layer was more rugged when plated at low frequency. From Figure 6e, it can be noted that increasing the frequency results in an increase in the crystallite size but a decline in the diameter. In order to explain the influence of frequency, by expressing the nucleation rate through current I, the relationship between three-dimensional nucleation rate and the overpotential is illustrated in the formula below [17]:

$$InI = A - B/\eta^2 \quad (2)$$

where A and B are constant, and η is the overpotential. Following this relation, as the overpotential increases, the speed of new crystal nucleus creation will also increase leading to a decrease in the crystallite size. If a certain quantity of new grains is formed rapidly, then more compact delicate deposits are obtained. When the frequency increases from 50 Hz to 800 Hz, it means that both T_{on} and T_{off} decrease in a cycle. Our experiments agree with previous results as mentioned by Yuan [17], in which he found that as the T_{on} in a cycle fell, the overpotential also fell and the crystallite size of the deposits increased.

XRD patterns were chosen to investigate the effect of duty cycle (ϕ) on nickel deposition. As shown in Figure 7, with an increase in the duty cycle from 33% to 67%, the (111) texture was still the preferred orientation of the deposits.

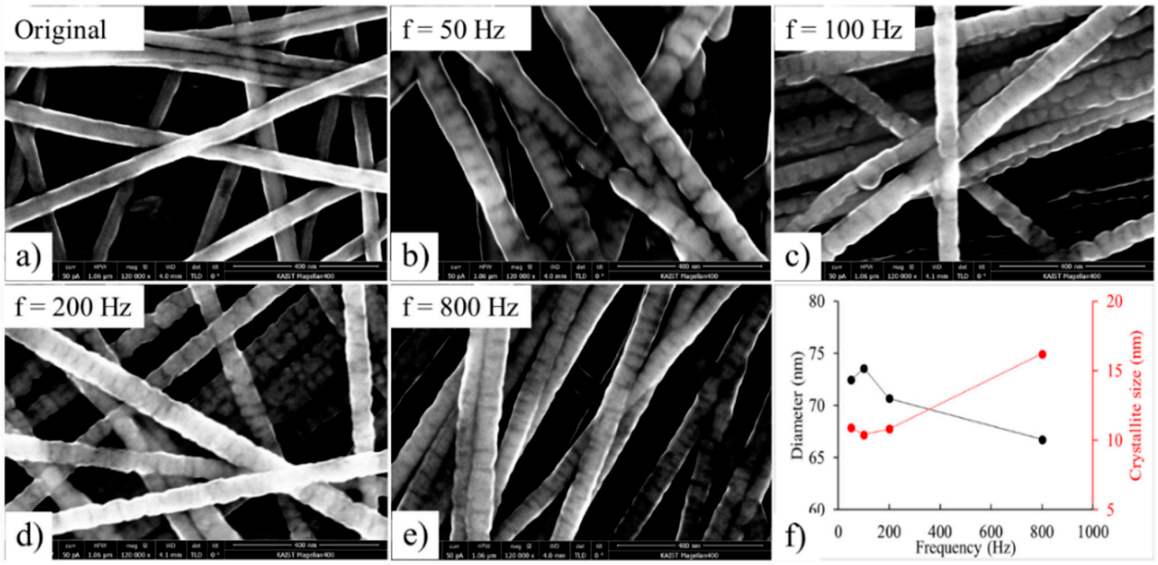

Figure 6. Influence of frequency on the surface morphology of nickel deposits with constant supplied power generated of 0 V–3 V and plating time of 90 s: (**a**) original Cu NWs; (**b**) f = 50 Hz; (**c**) f = 100 Hz; (**d**) f = 200 Hz; (**e**) f = 800 Hz; (**f**) diameter of wires and crystallite size after nickel plating at various frequencies.

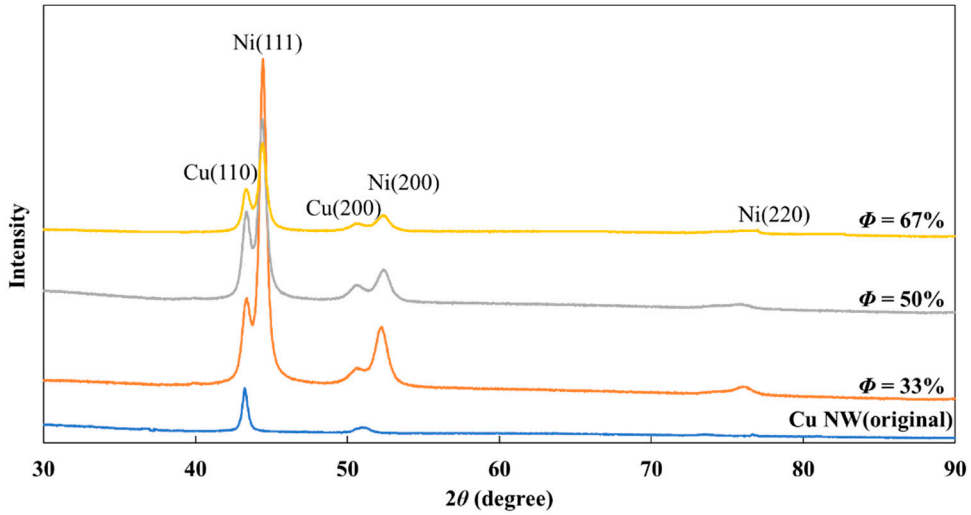

Figure 7. XRD patterns showing the influence of duty cycle (ϕ) on the crystal orientation of nickel deposits for an average applied voltage of 1.25 V.

Generally, transparent electrodes for industrial applications must exhibit acceptable uniformity. Practically, however, due to the effect of current distribution, it is very difficult to create a 100% uniform layer via the electroplating technique [18]. This study found that an even distribution can be achieved by selecting a suitable combination of frequency (f) and duty cycle (ϕ). These two factors are crucial for optimizing the electroplating process. To determine the optimum values, three criteria are considered:

(1) The difference of transmittances: $\Delta T = T_{after} - T_{before}$, (at a wavelength of 550 nm) of the Cu NW electrodes before and after plating.

(2) The difference of sheet resistances: $\Delta R = R_{after} - R_{before}$ of the Cu NW electrodes before and after plating.

(3) The uniformity of the electrodes after plating, which can be evaluated by observing and measuring the transparency at different positions on the Cu–Ni NW electrodes.

In an attempt to optimize the frequency and duty cycle (ϕ) in the plating process, fifteen Cu NW electrodes with an original transparency of 83% and sheet resistance of 20 Ω/sq were prepared. These samples were plated for 90 s under supplied power generated with a pulse of 0 V–3 V. A range of frequencies from 50 to 800 Hz and 3 different duty cycles (ϕ) of 33.3%, 50%, and 66.7% were investigated. Figure 8a shows the difference in sheet resistance before and after pulsed electrodeposition of Ni; all the electrodes were conductive, proving that the wires were connected over the entire film. However, at a duty cycle of 33.3%, because the plating efficiency was too low to cover the nanowire junctions completely, some areas in the NW network were deformed, which led to a decrease in the conductivity of the plated electrodes. When the duty cycle was increased to 50% and 66.7%, the sheet resistance decreased significantly. In both cases of 50% and 66.7%, the Cu–Ni NW films obtained the lowest sheet resistance after plating at a frequency of 400 Hz. However, the electrodes plated with ϕ = 50% had more uniform sheet resistance than those plated at ϕ = 66.7%. As shown in Figure 8b, the transmittance of the nickel-coated electrodes is almost equivalent to the original Cu NW electrodes, which makes it appear as though no nickel was deposited on the Cu NWs. In fact, the decline in transparency was found to be about 10% in the case of plating at ϕ = 50% and 20% with ϕ = 66.7%. To achieve an even distribution of nickel as well as greater efficiency, plating at ϕ = 50% and f = 400 Hz were mainly used in our subsequent studies.

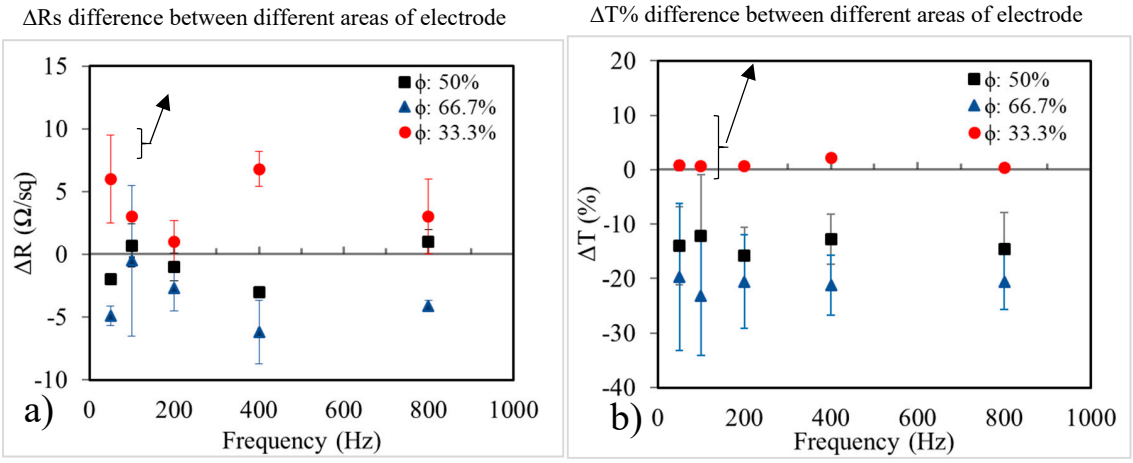

Figure 8. The change in (**a**) sheet resistance—ΔR and (**b**) transmittance—ΔT after nickel plating with various frequencies (f) and duty cycles (ϕ).

3.3. Influence of Current Density on Nickel Deposition

Normally, the conductivity of the Cu NW network will improve after plating with nickel, but this is accompanied by a reduction in the transmittance. However, some samples not only declined in transparency, but also decreased in conductivity. As an example, the sheet resistance of the Cu NWs electrodes increased from 18 Ω/sq to 22 Ω/sq, though the transmittance reduced 7%, from 86% to 79%. At the same time, we discovered a Cu NW which was disconnected by a crack after nickel plating. We considered that the reason for resistance increasing is probably cracking of the Cu NW network due to internal stress. During electroplating, internal stress plays a vital role in facilitating crack-free deposition. Due to the effect of electro-crystallization generation or the co-deposition of impurities, particularly hydrogen and sulfur, the internal stress can be controlled through the amount of deposited nickel [19].

To investigate the complete coverage of the Cu NWs by Ni, the experiment had five samples, which were firstly plated by PC at five different average current densities and secondly heated on a hotplate at 150 °C for a number of hours. We restricted our analysis to temperatures below 150 °C because at temperatures greater than 160 °C, a layer of Cu_2O can overgrow the NiO layer on cupronickel and change the oxidation kinetics [20]. The sheet resistance data was limited to a range in which $\Delta R/R_0 < 1$,

because a doubling in the sheet resistance would be unacceptable for most applications. As shown in Figure 9a, at current densities higher than 0.07 mA/cm^2, the sheet resistance is constant after 8 h on the hot plate at 150 °C, indicating that the Cu NWs are fully covered by the Ni layer hence protecting the Cu NWs from oxidation at high temperature. After fully covering the Cu NWs, in order to determine the current density that caused the cracking due to excess deposition, as highlighted previously, eight samples were plated by pulsed average current densities ranging from 0.07 mA/cm^2 to 0.2 mA/cm^2. Consequently, Figure 9b shows ΔR and ΔT of the electrodes after plating. The electrodes that were plated at current densities below 0.17 mA/cm^2 exhibited a decrease in the sheet resistance while the sheet resistance increased when plating at current densities higher than 0.17 mA/cm^2. In fact, at 0.14 mA/cm^2 of current density, the sheet resistance decreased 7 Ω/sq and the transmittance decreased 9% at the same time. Moreover, Figure 9c illustrates that the Cu NW network plated Ni without cracks at 0.14 mA/cm^2 of current density. For current density of 0.18 mA/cm^2, the sheet resistance of the electrode increased 5 Ω/sq while the transmittance reduced 14% and the microscope image (Figure 9d) showed cracks areas in Cu NW network. Furthermore, without Ni plating, the sheet resistance of the original Cu NW electrodes significantly increased to 200 Ω/sq after only 15 days. After the Ni plating process, the sheet resistance of electrodes in ambient conditions was not changed during 30 days. The effect of sheet resistance on the performance of the Cu–Ni NWs over a period of 30 days demonstrated the ability of Ni plating to act as a protective layer to shield the Cu NWs when exposed to air.

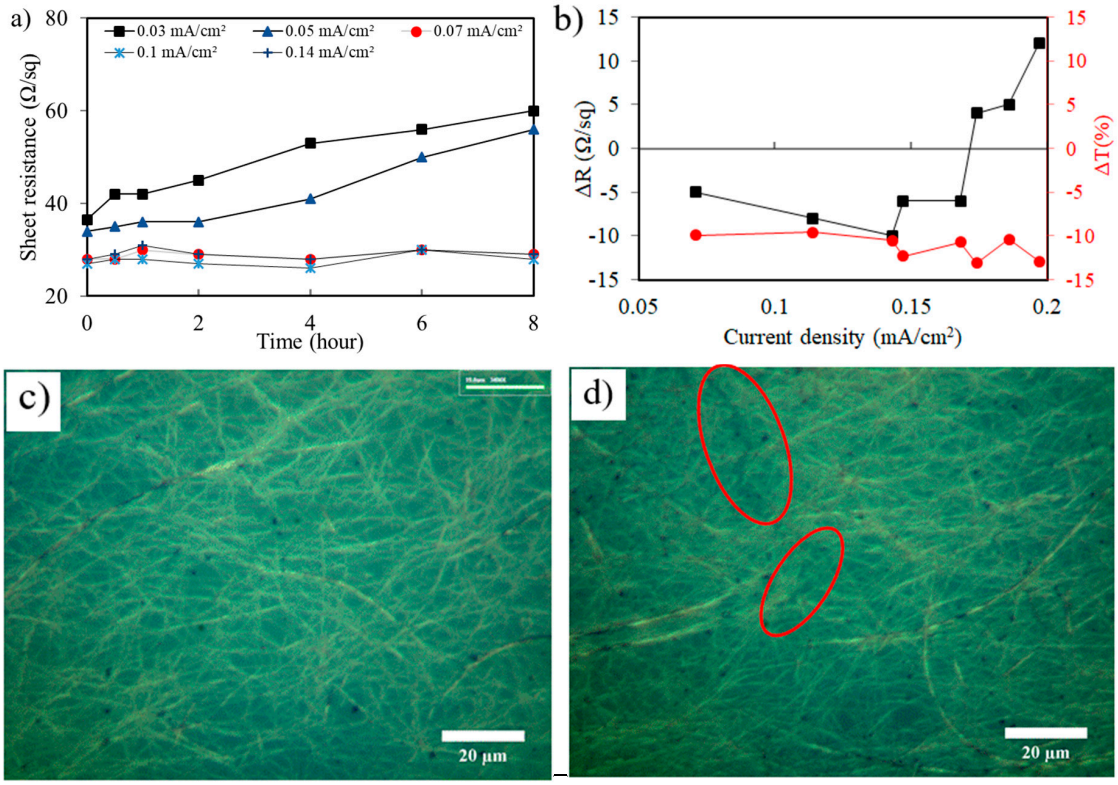

Figure 9. (**a**) The change in the sheet resistance of Cu–Ni NW electrodes which are plated at different average currents (mA/cm^2) while heating at 150 °C on a hot plate for 8 h (**b**) the change in the sheet resistance and transmittance of the electrode when an increasing current density is applied during PC plating, (**c**) microscope image showing an absence of cracks, (**d**) microscope image of cracks (red circle) as a result of PC plating at current density of 0.14 mA/cm^2 and 0.18 mA/cm^2, respectively.

3.4. Flexible Smart Window Fabrication

The mechanical flexibility of Cu–Ni on a PET substrate was investigated by the bending test system with bending radius R = 5 mm and frequency of 0.7 Hz. Two electrodes of Cu NWs and

Cu–Ni NWs, which had a sheet resistance of 32, and 27 Ω/sq and a transmittance of 85%, and 76%, respectively, were prepared. Figure 10a shows them during the bending process from the original state to the bent state then during recovery to the initial state. The electrodes coated on the PET substrate that had a thickness of 50 μm were bent in the middle of the surface. The change of sheet resistance of the two electrodes after the bending test is shown in Figure 10b. During the test, where R_0 is the initial measured resistance, the change in resistance ($\Delta R = R - R_0$) was measured for each sample, and R is the resistance measured under bending. As can be seen in Figure 10b, both the sheet resistance of the Cu NWs and Cu–Ni NWs electrodes increased slightly when bending in the first 4000 cycles. Subsequently, when the number of cycles increased up to 6000, the sheet resistance of the Cu NW electrodes increased significantly due to delamination, whereas there was only a slight increase in the sheet resistance of the Cu–Ni NW electrodes. As a result, the Cu–Ni NWs exhibit high flexibility, making them quite appropriate for various applications in which flexibility is important.

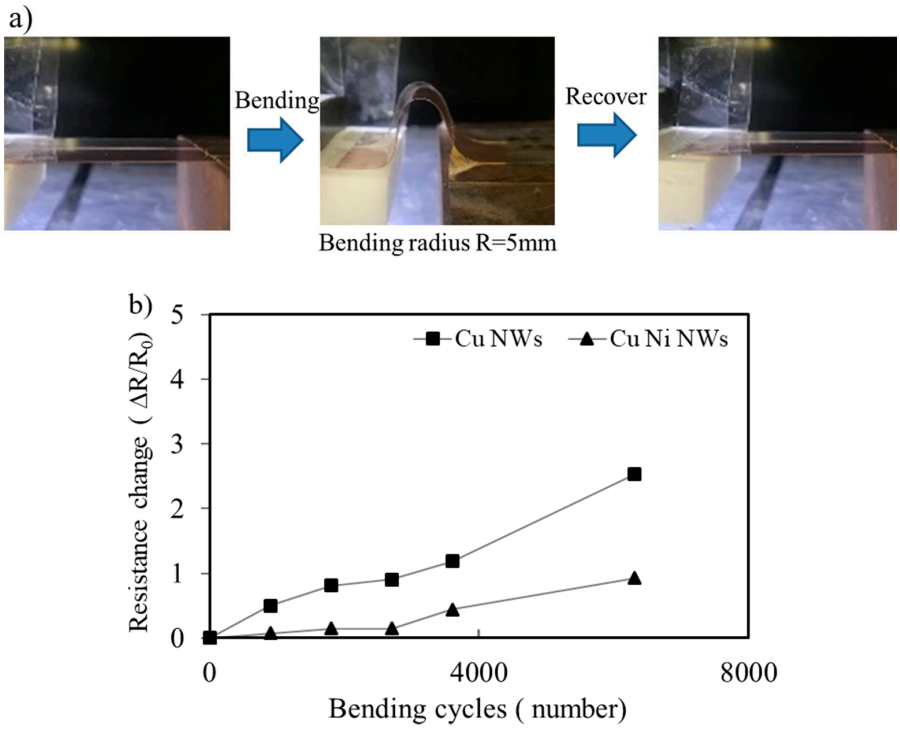

Figure 10. (**a**) The images of the bending and recovery process with a bending radius, R = 5 mm and (**b**) the chart of the number of repeating bending cycles with the change in resistance ($\Delta R/R_0$).

Figure 11 shows the photographs of flexible PDLC smart windows with 2 Cu–Ni electrodes on PET film prepared by PC plating in the "ON state" and "OFF state". They had a sheet resistance of 27 Ω/sq and a transmittance of 76% at a wavelength of 550 nm. In fact, the reddish color of Cu NW electrodes makes them unsuitable for optical applications. Therefore, a change to using the gray color of the Cu–Ni NWs electrodes as shown in Figure 11 was an appropriate solution. The operation of the smart windows is illustrated by the schematic in Figure 2 and photographs in Figure 11. When voltage was applied, the opaque state immediately changed to the transparent state. This can be explained because the "OFF state" reduces the passage of light through to the polymer layer due to randomly oriented microdroplets. In the "ON state", the light can be transmitted through the PDLC smart window because of the alignment of the microdroplets, therefore the text line behind the window is seen more clearly. Moreover, the window operated normally when the voltage was applied in the bending state, hence demonstrating the suitability and potential use of the Cu–Ni NW electrodes in flexible applications.

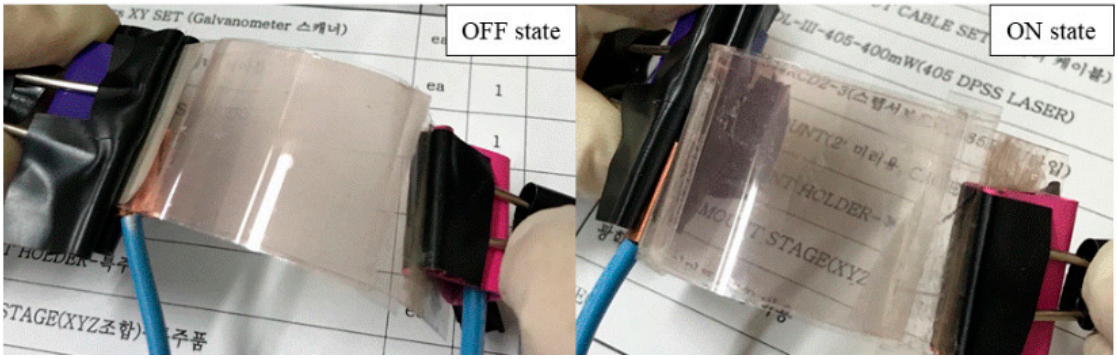

Figure 11. Photographs of Cu–Ni electrode-based flexible PDLC smart windows at 2 states: OFF state and ON state.

Figure 12a shows the transmittance of the Cu–Ni NW-based PDLC smart window in the "ON" and "OFF" states as a function of wavelengths from 350 nm to 800 nm. As a result, the difference in transparency at 550 nm between the on- and off-state for the nanowire-based device, ΔT_{on-off} was 47.5% (69% in the on-state and 21.5% in the off-state). Moreover, as shown in Figure 12b, the transmittance of the window increased when the applied voltage was increased and reached 90% of its maximum transmittance at 50 V. As a result, the windows exhibited a transmittance of 63% using an applied voltage of 50 V.

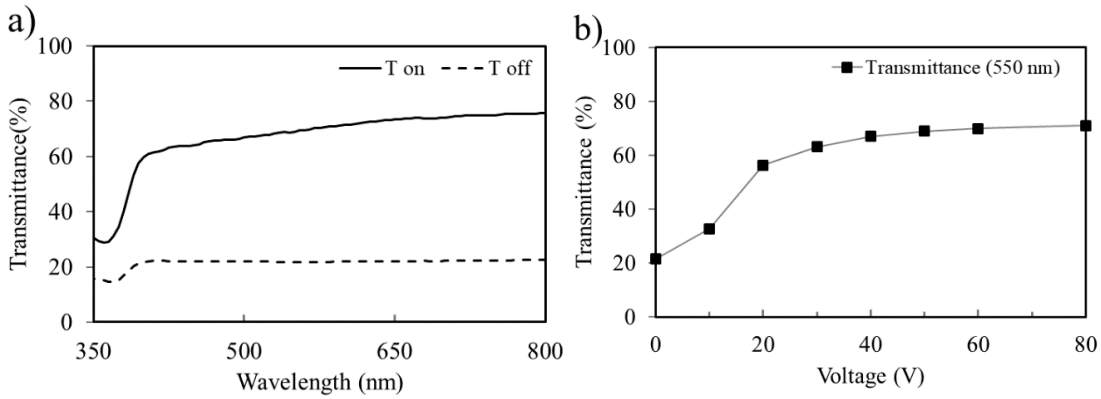

Figure 12. (**a**) The optical transmittance of the Cu–Ni NWs in the "ON" and "OFF" states for wavelengths ranging from 350 to 850 nm. (**b**) The transmittance of the Cu–Ni NW-based PDLC smart window with increasing applied voltage at 550 nm.

4. Conclusions

The pulsed nickel-plating method developed here shows great promise as an electroplating method that permits modifying parameters such as duty cycle and frequency to enhance the performance of the Cu NWs. The nickel layers covered the Cu NWs effectively, protecting them from oxidation, and hence facilitating enhanced stability of the electrodes when exposed to air over a period of 30 days. Moreover, the conductivity of the Cu–Ni network was improved after solving the problem of crack development resulting from excessive deposition. The gray color, and the maintenance of low sheet resistance after the 6000 bending cycle test was performed on the flexible PDLC smart window, demonstrate the tremendous potential use of the Cu–Ni NW electrodes in optical applications.

Author Contributions: The manuscript was written through contributions of all authors. All authors have given approval to the final version of the manuscript.

Funding: This research was supported by Basic Science Research Program through the National Research Foundation of Korea (NRF) funded by the Ministry of Education (2017R1D1A1B03029074).

Acknowledgments: We are immensely grateful to Thanh-Hung Duong for supporting us.

Conflicts of Interest: The authors declare no conflict of interest.

References

1. Ye, S.; Rathmell, A.R.; Chen, Z.; Stewart, I.E.; Wiley, B.J. Metal nanowire networks: The next generation of transparent conductors. *Adv. Mater.* **2014**, *26*, 6670–6687. [CrossRef] [PubMed]
2. Ye, S.; Rathmell, A.R.; Stewart, I.E.; Ha, Y.-C.; Wilson, A.R.; Chen, Z.; Wiley, B.J. A rapid synthesis of high aspect ratio copper nanowires for high-performance transparent conducting films. *Chem. Commun.* **2014**, *50*, 2562–2564. [CrossRef] [PubMed]
3. Rathmell, A.R.; Wiley, B.J. The synthesis and coating of long, thin copper nanowires to make flexible, transparent conducting films on plastic substrates. *Adv. Mater.* **2011**, *23*, 4798–4803. [CrossRef] [PubMed]
4. Chu, C.R.; Lee, C.; Koo, J.; Lee, H.M. Fabrication of sintering-free flexible copper nanowire/polymer composite transparent electrodes with enhanced chemical and mechanical stability. *Nano Res.* **2016**, *9*, 2162–2173. [CrossRef]
5. Chen, Z.; Ye, S.; Stewart, I.E.; Wiley, B.J. Copper nanowire networks with transparent oxide shells that prevent oxidation without reducing transmittance. *ACS Nano* **2014**, *8*, 9673–9679. [CrossRef] [PubMed]
6. Deng, B.; Hsu, P.C.; Chen, G.; Chandrashekar, B.N.; Liao, L.; Ayitimuda, Z.; Wu, J.; Guo, Y.; Lin, L.; Zhou, Y.; et al. Roll-to-Roll Encapsulation of Metal Nanowires between Graphene and Plastic Substrate for High-Performance Flexible Transparent Electrodes. *Nano Lett.* **2015**, *15*, 4206–4213. [CrossRef] [PubMed]
7. Won, Y.; Kim, A.; Lee, D.; Yang, W.; Woo, K.; Jeong, S.; Moon, J. Annealing-free fabrication of highly oxidation-resistive copper nanowire composite conductors for photovoltaics. *NPG Asia Mater.* **2014**, *6*, e105. [CrossRef]
8. Chao, J.F.; Meng, Y.Q.; Liu, J.B.; Zhang, Q.Q.; Wang, H. Review on the Synthesis and Antioxidation of Cu Nanowires for Transparent Conductive Electrodes. *Nano* **2019**, *14*, 1930005. [CrossRef]
9. Chen, Z.; Rathmell, A.R.; Ye, S.; Wilson, A.R.; Wiley, B.J. Optically transparent water oxidation catalysts based on copper nanowires. *Angew. Chem. Int. Ed.* **2013**, *52*, 13708–13711. [CrossRef] [PubMed]
10. Duong, T.H.; Hoang, H.M.; Kim, H.C. An investigation of electrical nickel deposition on copper nanowires-based electrodes. *Chem. Eng. Commun.* **2019**, 1–13. [CrossRef]
11. Rathmell, A.R.; Nguyen, M.; Chi, M.; Wiley, B.J. Synthesis of Oxidation-Resistant Cupronickel Nanowires for Transparent Conducting Nanowire Networks. *Nano Lett.* **2012**, *12*, 3193–3199. [CrossRef] [PubMed]
12. Duong, T.-H.; Kim, H.-C. An extremely simple and rapid fabrication of flexible transparent electrodes using ultralong copper nanowires. *Ind. Eng. Chem. Res.* **2018**, *57*, 3076–3082. [CrossRef]
13. Sharma, R.K.; Singh, G.; Rastogi, A.C. Pulsed electrodeposition of CdTe thin films: Effect of pulse parameters over structure, stoichiometry and optical absorption. *Sol. Energy Mater. Sol. Cells* **2004**, *82*, 201–215. [CrossRef]
14. Chandrasekar, M.S.; Pushpavanam, M. Pulse and pulse reverse plating-Conceptual, advantages and applications. *Electrochim. Acta* **2008**, *53*, 3313–3322. [CrossRef]
15. Wu, H.; Hu, L.; Rowell, M.W.; Kong, D.; Cha, J.J.; McDonough, J.R.; Zhu, J.; Yang, Y.; McGehee, M.D.; Cui, Y. Electrospun metal nanofiber webs as high-performance transparent electrode. *Nano Lett.* **2010**, *10*, 4242–4248. [CrossRef] [PubMed]
16. Zhang, D.; Wang, R.; Wen, M.; Weng, D.; Cui, X.; Sun, J.; Li, H.; Lu, Y. Synthesis of ultralong copper nanowires for high-performance transparent electrodes. *J. Am. Chem. Soc.* **2012**, *134*, 14283–14286. [CrossRef] [PubMed]
17. Xuetao, Y.; Yu, W.; Dongbai, S.; Hongying, Y. Influence of pulse parameters on the microstructure and microhardness of nickel electrodeposits. *Surf. Coat. Technol.* **2008**, *202*, 1895–1903. [CrossRef]
18. Di Bari, G.A. Electrodeposition of Nickel. *Mod. Electroplat.* **2011**, *5*, 79–114.
19. Chen, F.J.; Pan, Y.N.; Lee, C.Y.; Lin, C.S. Internal stress control of nickel-phosphorus electrodeposits using pulse currents. *J. Electrochem. Soc.* **2010**, *157*. [CrossRef]
20. Castle, J.E.; Nasserian-Riabi, M. The oxidation of cupronickel alloys-I. XPS study of inter-diffusion. *Corros. Sci.* **1975**, *15*, 537–543. [CrossRef]